Journal of Radioanalytical and Nuclear Chemistry (2019) 319:695–701
https://doi.org/10.1007/s10967-018-6368-1

Measurements of ^{60}Ni(p,n)^{60}Cu reaction cross-sections and covariance analysis of the uncertainty

B. Lawriniang[1] · R. Ghosh[1] · S. Badwar[1] · Santhi Sheela Yerraguntla[2] · B. Jyrwa[1] · H. Naik[3] · Y. P. Naik[4] · S. V. Suryanarayana[5]

Received: 23 July 2018 / Published online: 10 December 2018

Abstract

The cross sections of the ^{60}Ni(p,n)^{60}Cu reaction from threshold energy to ~ 20 MeV have been measured by employing stack foil activation technique and off-line γ-ray spectrometry. The uncertainties for the reaction cross sections have been estimated by applying covariance analysis and least square method. The measured cross-sections are found to be in agreement with most of the literature data available in EXFOR database. The excitation function of the ^{60}Ni(p,n)^{60}Cu reaction was also theoretically calculated by using the TALYS-1.9 code. The excitation functions of ^{60}Ni(p,n)^{60}Cu reaction from TALYS-1.9 and TENDL-2017 follow a similar trend as of the experimental data of present work and literature but are little higher around the peak cross-section region.

Keywords ^{60}Ni(p,n)^{60}Cu reaction · γ-Ray spectroscopy · Reaction cross-section · Covariance analysis · TALYS-1.9 · TENDL-2017

Introduction

Nickel is one of the structural materials that are frequently used in alloys due to its anti-corrosion property. The experimental measurements of charged particle induced reactions are necessary for understanding the nuclear structure, nuclear excited state properties and also to measure the nuclear processes in a reactor [1, 2]. The interaction of charged particle and in particularly proton induced reactions are more challenging as compared to neutron and photon induced reactions as it has to overcome the coulomb barrier and rapidly loses energy within the target. The Coulomb barrier prevents any appreciable interaction with the nucleus at low energies. The proton induced reaction cross section of nickel has a wide range of applications in nuclear and space technology and in the development of an accelerator driven sub-critical system (ADSs) [3]. It also plays an important role for the production of medical isotopes such as ^{60,61,62}Cu and ^{55,56,57,58}Co etc. Medical radioisotopes can be produced either using particle accelerators or nuclear reactors. These radioisotopes have been widely used in diagnostic investigation especially in single photon emission computed tomography (SPECT) and positron emission tomography (PET) as well as in endo-radiotherapy [2]. One of the most important applications of proton therapy is in cancer treatment. However, charged particles transfer most of their energy to the tumor, but they also transfer energy to the surrounding normal tissues thus resulting in a dose penumbra [4]. ^{60}Cu is one of the medical isotopes that is usually used as PET radionuclides [5]. Its decay characteristic and a half-life of 23.7 min makes it one of the potential radionuclides for molecular imaging and radiotherapy since large amount of activity can be administered for good counting in short period of time and also maintaining a fairly low total absorbed radiation dose.

The literature survey shows that although considerable cross sections data for the ^{60}Ni(p,n)^{60}Cu reaction are

✉ H. Naik
naikhbarc@yahoo.com

1 Physics Department, North Eastern Hill University, Shillong, Meghalaya 793022, India

2 Department of Statistics, Manipal University, Manipal 576104, India

3 Radiochemistry Division, Bhabha Atomic Research Center, Trombay, Mumbai 400085, India

4 Product Development Division, Bhabha Atomic Research Centre, Trombay, Mumbai 400085, India

5 Nuclear Physics Division, Bhabha Atomic Research Center, Trombay, Mumbai 400085, India

available in literature [6–10], there is some disagreement between the literature data and the theoretical prediction. Moreover, the experimental data by Singh et al. [8] and Blosser et al. [7] have large uncertainties. This may be because they have measured only the standard deviation or variances, which would be correct only if all the variables are completely independent of each other. If they are related then the covariance comes into play, which measures the uncertainty in the data contributed by more than one attributes that are inter-dependent on each other.

In view of the above facts, the cross-sections of ^{60}Ni(p,n)^{60}Cu reaction from threshold energy to ~ 20 MeV have been measured by taking proper care of the uncertainties. It is a well-known fact that the experimental measurements are not always same as theoretical values and are always subjected to measurement uncertainties. Thus the covariance analysis [11] for the uncertainty is being done in this work to study the occurrence of errors and hence increase the accuracy and reliability of the final reaction cross-sections. The analysis is done by evaluating the effects of partial uncertainties from the individual parameters, taking into account the correlation of uncertainties between input data, on the uncertainty in the resulted cross-sections. The obtained experimental cross-section of the ^{60}Ni(p,n)^{60}Cu reaction were then compared with the literature data available in EXFOR database [12] as well as with the theoretical values based on nuclear code TALYS-1.9 [13] and TENDL-2017 [14] data library.

Experimental details

The general features and techniques for irradiation, activity assessment and the reaction cross-section determination in this work are similar to those of our previous work [15]. All the experimental specifications and details are summarised in Table 1 and are briefly discussed here.

For the measurement of ^{60}Ni(p,n)^{60}Cu reaction cross-section, experiment was performed by using the 14UD BARC-TIFR (Bhabha Atomic Research Centre and Tata Institute of Fundamental Research) Pelletron facility [16] at Mumbai, India. The radionuclide ^{60}Cu was produced by the well-known stacked foil activation technique and its gamma-ray activity was measured by using an off-line gamma-ray spectrometry. High purity (> 99.99%) nickel foils of thickness 101 µm and dimensions 0.7 × 0.7 cm^2, arranged as given in Table 1 were used as the target for irradiation. Also, high purity (> 99.99%) copper foils of thickness 99 µm were sandwiched in between the nickel foils samples alternately, to monitor the proton beam intensity. In order to avoid contamination from other samples, each foil was wrapped with aluminium foil of 25 µm thick. The stack consists of five nickel target foils within the proton energy range from 7.25 ± 1.39 to 18.88 ± 0.76 MeV. The stack of foils was irradiated with a proton beam of 20 MeV in the main line at 6 m above the analysing magnet of the Pelletron facility. The irradiation lasted for 10 min with a beam current of 100 nA. The copper foils were irradiated simultaneously with the nickel foils. The ^{nat}Cu(p,x)^{62}Zn reaction, of known cross-section taken from recommended IAEA database [17], was

Table 1 Experimental description of present work

Accelerator used	BARC-TIFR Pellatron facility, Mumbai [16]
Primary energy	20 MeV
Range of the proton energy (MeV)	7.25–18.88 MeV
Stack arrangement	Ni–Cu–Ni–Cu–Ni–Cu–Ni–Cu–Ni–Cu wrapped with 25 µM thick Al foil
Method	Stacked foil activation and off-line γ-ray spectrometry
Target, thickness and size	^{nat}Ni foils (> 99.99% purity), 101 µm thick and 0.7 × 0.7 cm^2 in area
Number of target foils	Five
Irradiation time	10 min
Beam current	100 nA
Monitor target, thickness and size	^{nat}Cu (> 99.99% purity), 25 µm thick and 0.8 × 0.8 cm^2 in area
Monitor reaction based on IAEA database [17]	^{nat}Cu(p,x)^{62}Zn reaction
Monitor proton energy and Cross-section	17.34 ± 0.78 MeV, 33.61 mb
Detector	HPGe
Calibration source	^{152}Eu [18]
Cooling times	1.05–1.58 h
Decay data	NuDat 2.7β [19], Livechart [20]
Reaction Q-values	Q-value calculator [21]
Determination of beam energy	SRIM-2013 [22]

used as the monitor reaction. At the same time, the copper foils also serve as the energy degrader along the stack. The energy of the incident proton beam decreases as it passes along the stack, therefore each foil was irradiated with different proton energies. This degradation in the beam energy along the stack was calculated using the computer program SRIM 2013 [22], which is based on the formulas and tables of Anderson and Ziegler. The beam intensity was kept constant during the irradiation and it was found that the loss of proton flux along the stack was very small or negligible. Therefore, the proton beam intensity was considered as constant throughout the stack.

After the end of irradiation, the samples were mounted on different Perspex plates of particular size, which fits on the shelf of the sample stand. Then the γ-ray activity of ^{60}Cu produced from the nickel foils was measured with a high resolution HPGe detector connected to a PC based 4 K channel analyser. The energy and efficiency calibration of HPGe detector was done using the ^{152}Eu [18] standard point source of known activity. The γ-ray activity of ^{62}Zn produced from the irradiated copper monitor foils were also counted with the same detector and in a same geometry. The measurements of γ-ray activities from each activated foils were started after a sufficient cooling times of 1.05–1.58 h. The measurements were done at a distance of 15 cm from the end cap of the detector to keep the dead time as minimum as possible. The radioactive products ^{60}Cu from the ^{60}Ni(p,n) reaction and ^{62}Zn from the ^{nat}Cu(p,x) reaction were then identified by their characteristic γ-lines as well as by their measured half-lives.

Data analysis

In the present work, the cross-sections of ^{60}Ni(p,n)^{60}Cu reaction were measured at four proton energies from threshold up to 18.88 ± 0.76 MeV. This is because the proton energy faced by the last foil is only 4.05 MeV, which is below the threshold energy of 7.0269 MeV for the ^{60}Ni(p,n)^{60}Cu reaction. Since covariance analysis is being done, therefore the data analysis section is divided into two parts as (1) detector calibration and uncertainty in detector efficiency, (2) estimation of cross-section and its uncertainty.

Detector calibration and uncertainty in detector efficiency

The standard ^{152}Eu point source [18] of known activity was used for energy calibration as well as to obtain the efficiency of the HPGe detector for various characteristic γ-ray energies by placing the source at a distance of about 15 cm from the end cap of the detector. The energy-efficiency calibration was carried out in the detector placed at Tata Institute of Fundamental Research [16], Mumbai, whose energy resolution was 1.8 keV for the 1332.5 keV γ-line of ^{60}Co. The efficiency of the detector for the six characteristics γ-lines were determined by using Eq. (1). The six γ-ray energies of standard ^{152}Eu source considered in this calculations are 121.8, 244.7, 344.3, 778.9, 1112.1 and 1408.0 keV.

$$\varepsilon = \frac{C_{cps}}{A_0 e^{-\left(\frac{0.693T}{T_{1/2}}\right)} I_\gamma} \quad \text{where} \quad C_{cps} = \frac{C}{\Delta t} \tag{1}$$

where ε is the efficiency of the detector; C is the detected γ-ray counts measured in time Δt; I_γ is the γ-ray abundance; A_o is the activity of the ^{152}Eu point source; $T_{1/2}$ is the half-life of radioactive nuclei; T is the time between source and detector calibration.

The half-life and decay data of ^{152}Eu used in Eq. (1) were retrieved from Nudat [19] database. In Eq. (1), the parameters T and Δt were measured without any uncertainty related to them, therefore we consider efficiency to be a function of these four attributes i.e. $\varepsilon = \varepsilon(C, I_\gamma, A_0, T_{1/2})$. All the four attributes are measured independently i.e.no correlation exist among the attributes. The total uncertainty in efficiency is obtained by propagating the uncertainty on the counts (C), the γ-ray abundance (I_γ), the point source activity (A_0) and half-life ($T_{1/2}$) where the partial uncertainties in efficiency $\varepsilon_{(E_i)}$ due to each attribute x_a at energy E_i are given by

$$\delta_{(E_i)a} = \left| \frac{\partial \varepsilon_{(E_i)}}{\partial x_a} \right| \delta x_a \tag{2}$$

By using the law of error propagation, the uncertainty in efficiency is given as [23, 24]

$$\delta_{(E_i)a} = \sqrt{\sum_{a=1}^{4} \delta^2_{(E_i)a}}, \quad 1 \le i \le 6, \tag{3}$$

The covariance matrix $(C_\varepsilon)_{ij}$ representing the uncertainties in the measured efficiencies due to the ith and jth γ-line is given by

$$(C_\varepsilon)_{ij} = \sum_{a=1}^{4} \delta_{(E_i)a} (M_\varepsilon)_{ija} \delta_{(E_j)a}, \quad 1 \le i,j \le 6 \tag{4}$$

where $(M_\varepsilon)_{ija}$ is the micro-correlation matrix of order 6 × 6. $(M_\varepsilon)_{ija}$, is denoted by an identity matrix or a matrix of 1's in case of independent or fully correlated data, respectively.

In order to obtain the most accurate values, the efficiency calibration curve was fitted to a polynomial function. The linear parametric model of order m and estimated fitting parameters b_{m-1} can be expressed as $\ln \varepsilon_i = \sum_{m=1}^{l} b_{m-1} (\ln E_i)^{m-1}$. The corresponding linear model of the above equation can be represented in matrix form as $Z_{6x1} \approx A_{6xm}B_{mx1}$, where $Z_i = ln\varepsilon_i$ is a column matrix. A is a matrix of natural logarithmic of γ-lines E_i's with elements $A_{il} = ln(E_i)^{l-1}, 1 \le l \le m; 1 \le k \le 6$ and B is the column matrix of parameters b_{m-1} to be estimated. On conversion of $(C_\varepsilon)_{ij}$ to $(C_z)_{ij}$, the final C_z matrix takes the form $(C_z)_{ij} = \frac{(C_\varepsilon)_{ij}}{\varepsilon_i\varepsilon_j}$. A good fit measuring the consistency of the data is tested by Chi square statistic, χ^2 which is given by $\chi^2 = (Z - AB)^T C_z^{-1}(Z - AB)$, where the superscript "− 1" denotes the inverse and "T" the transpose of a matrix. From the least square method [25, 26], the best estimate B of the solution parameters is obtained by solving $\frac{d\chi^2}{dB} = 0$, which leads to $B = \left(A^T C_z^{-1} A\right)^{-1} A^T C_z^{-1} Z$ and its covariance matrix is in turn given by $C_B = \left(A^T C_z^{-1} A\right)^{-1}$.

For the efficiency calibration, the best fit using least square method was obtained for a second order polynomial with parametric equation ln $\varepsilon = -7.993 - 0.948$ (ln E) and $\frac{\chi^2}{(n-m)} = 0.95$. Since the γ-ray energies (E_c) of the radioactive products are not the same as the calibrated energy lines (E_i), therefore the efficiencies of the γ-lines of radioactive nuclides with energies E_c can be estimated by interpolation using least square method [25]. The final covariance information of Z_c denoted by C_{Zc} was again calculated by employing the error propagation formula $C_{zc} = A_c^T C_B A_c$ with elements $A_{ci} = (\ln E_{ci})^{l-1}$. Hence,$(C_{\varepsilon c})_{ij} = (\varepsilon_c)_i (C_{zc})_{ij} (\varepsilon_c)_j$

The estimated efficiencies at the characteristics γ-rays of the reaction products ^{60}Cu and ^{62}Zn along with the correlation matrix defined as $Corr\varepsilon(i,j) = \frac{(C_{\varepsilon c})_{ij}}{\sqrt{(C_{\varepsilon c})_{ii}(C_{\varepsilon c})_{jj}}}$ are given in Table 2.

Table 2 Interpolated detector efficiencies of the radionuclide with its correlation matrix

Radionuclide	γ-line energy (keV)	Efficiency	Correlation matrix	
^{62}Zn	596.6	5.515E−04 ± 1.930E−05	1	
^{60}Cu	1332.5	2.574E−04 ± 1.359E−05	0.916	1

Estimation of ^{60}Ni(p,n)^{60}Cu reaction cross-section with its uncertainty

The cross-section for the ^{60}Ni(p,n)^{60}Cu reaction from threshold energy up to 18.88 ± 0.76 MeV were calculated using the activation formula [27]

$$\sigma_R = \frac{C_{Ni} Avm_{Ni} W_{Cu} \sigma_{Cu} I_{\gamma_{Cu}} \varepsilon_{Cu} f_{\lambda_{Cu}}}{C_{Cu} Avm_{Cu} W_{Ni} a_{Ni} I_{\gamma_{Ni}} \varepsilon_{Ni} f_{\lambda_{Ni}}} \quad (5)$$

where C is the net counts in the photo-peak; Avm is the average mass; W is the weight of the sample; a is the isotopic abundance; I_γ is the branching intensity; ε is its detection efficiency; σ_{Cu} is the monitor reaction cross-section taken from IAEA database [17]

$$f_\lambda = \frac{\lambda}{\left(1 - e^{-\lambda T_i}\right) e^{-\lambda T_c} \left(1 - e^{-\lambda \Delta T}\right)} \text{ is the time factor} \quad (6)$$

λ is the decay constant ($\lambda = \frac{ln2}{T_{1/2}}$) of the reaction product of interest with a half-life $T_{1/2}$

T_i, T_c, and ΔT are the irradiation, cooling and counting times, respectively.

The subscripts Ni and Cu in Eq. (5) signify the target and monitor, respectively. The decay and spectrometric characteristics of the activated products were taken from NuDat [19] database and chart of nuclides-IAEA Nuclear Data Services [20], which are summarised in Table 3 together with the Q-value [21] of the contributing reactions.

As shown in Table 1, the copper foil which was placed in second position after nickel foil in the stack arrangement (i.e. the first Cu foil) was used for proton flux determination via the ^{nat}Cu(p,x)^{62}Zn monitor reaction with known cross-section available in IAEA database [17]. No uncertainty was attributed to the monitor cross section due to lack of information from the database [17]. The proton beam loses energy as it travel along the stack and this energy degradation was calculated using the computer code SRIM 2013 [22], which is based on the energy range relation describe by Anderson and Ziggler. The loss of proton flux along the stack was negligibly small and therefore it was treated as a constant throughout the stack [28, 29].

Table 3 Nuclear spectroscopic data for the radionuclides from the ^{nat}Cu(p,x)^{62}Zn and ^{60}Ni(p,n)^{60}Cu reactions

Nuclei	Half-life	Decay mode	γ-ray energy E_γ (keV)	γ-ray intensity I_γ (%)	Production route	Threshold energy (MeV)	Spin parity
^{62}Zn	9.186 ± 0.013 h	ε (100%)	596.6	26.0 ± 0.2	^{63}Cu(p,2n)	13.4756	0^+
^{60}Cu	23.7 ± 0.4 min	ε (100%)	1332.5	88 ± 1	^{60}Ni(p,n)	7.0269	2^+

The parameters C, λ, Avm, a, I_γ and ε in activation formula were observed with error. The uncertainties in T_i, T_c, ΔT and W were too small to be incorporated in the uncertainty of the final reaction cross-sections. As in the case of efficiency, the partial uncertainty in the cross-section σ_j at proton energy E_i due to attribute q, except for the time factor f_λ is propagated as

$$\delta_{(\sigma_j,E_i)q} = \left|\frac{\partial \sigma_{j,E_i}}{\partial x_q}\right| \delta x_q \tag{7}$$

For e.g., the value 4.360E−01 of C_{Ni} at proton energy 7.25 ± 1.39 MeV in Table 4 is obtained from Eq. (7) by taking the partial derivative with respect to C_{Ni} i.e.

$$\delta_{(\sigma_j,E_i)q} = \frac{\partial}{\partial C_{Ni}}\left(\frac{C_{Ni}Avm_{Ni}W_{Cu}\sigma_{Cu}I_{\gamma_{Cu}}\varepsilon_{Cu}f_{\lambda_{Cu}}}{C_{Cu}Avm_{Cu}W_{Ni}a_{Ni}I_{\gamma_{Ni}}\varepsilon_{Ni}f_{\lambda_{Ni}}}\right)\delta C_{Ni} = \frac{\sigma_j}{C_{Ni}}\delta C_{Ni} \tag{8}$$

Whereas, the uncertainty in time factor, f_λ is propagated as [28]

$$\left(\frac{\delta f}{f}\right)^2 = s_{f_\lambda}^2\left(\frac{\delta\lambda}{\lambda}\right)^2 \tag{9}$$

where $S_{f_\lambda} = \frac{\lambda}{f}\frac{\partial f}{\partial \lambda} = (\frac{\lambda T_i e^{-\lambda T_i}}{1-e^{-\lambda T_i}} - \lambda T_c + \frac{\lambda C L e^{-\lambda \Delta T}}{1-e^{-\lambda \Delta T}} - 1)$ is the relative sensitivity matrix.

The partial uncertainties and correlation in cross-section within the attributes from the two γ-lines are presented in Table 4. In the table, "0 and 1" signifies uncorrelated and fully correlated, respectively.

The final covariance matrix in the cross-section is obtained by using the following equation

$$C_\sigma = \sum_{i,j} \delta_{(\sigma,E_i)}(M_\sigma)_{ij}\delta_{(\sigma,E_j)} \tag{10}$$

The interpolated efficiencies for the γ-lines of the raionuclide ^{60}Cu produced from the ^{60}Ni(p,n) reaction and ^{62}Zn from the ^{nat}Cu(p,x) reaction were obtained from the same model. Therefore the two efficiencies are partially correlated and their degree of correlation is given in Table 2. Hence, the uncertainty in the final cross-section of this work is calculated as

$$\delta\sigma = \sqrt{\sum_1^6 \delta^2_{(\sigma,E_i)\mathrm{Ni}} + \sum_1^6 \delta^2_{(\sigma,E_i)\mathrm{Cu}} + 2\sum \delta_{(\sigma,E_i)\varepsilon_{Ni}} Corr(\varepsilon_{Ni},\varepsilon_{Cu})\delta_{(\sigma,E_i)\varepsilon_{Cu}}} \tag{11}$$

The final cross-sections of ^{60}Ni(p,n)^{60}Co reaction at four proton energies together with its correlation matrix are presented in Table 5.

Table 5 Final Reaction cross-section of ^{60}Ni(p,n)^{60}Cu reaction

Proton energy, E_p (MeV)	Reaction cross-section, σ_R (mb)	Correlation matrix			
7.25 ± 1.39	19.0 ± 2.4	1			
11.97 ± 1.03	284.2 ± 35.6	0.957	1		
15.70 ± 0.85	150.2 ± 18.9	0.952	0.961	1	
18.88 ± 0.76	47.7 ± 6.0	0.952	0.954	0.948	1

Table 4 Partial uncertainties and correlation in cross-section within the attributes

	Proton energy, (MeV) Attributes	7.25	11.97	15.70	18.88	Correlation
Counts	C_{Cu}	7.807E−01	1.165E+01	6.610E+00	1.955E+00	1
	C_{Ni}	4.360E−01	2.728E+00	1.838E+00	7.046E−01	0
γ-intensity	$I_{\gamma_{Cu}}$	1.465E+00	2.186E+01	1.156E+01	3.669E+00	1
	$I_{\gamma_{Ni}}$	2.164E−01	3.229E+00	1.707E+00	5.420E−01	1
Isotopic abundance	a_{Cu}	4.131E−02	6.164E−01	3.259E−01	1.035E−01	1
	a_{Ni}	5.807E−03	8.666E−02	4.582E−02	1.454E−02	1
Average mass	Avm_{Cu}	8.990E−04	1.341E−02	7.093E−03	2.2528−03	1
	Avm_{Ni}	6.489E−05	9.683E−04	5.120E−04	1.625E−04	1
Efficiency	ε_{Cu}	6.663E−01	9.943E+00	5.257E+00	1.669E+00	1
	ε_{Ni}	1.005E+00	1.500E+01	7.932E+00	2.518E+00	1
Time factor	f_{Cu}	2.350E−02	3.507E−01	1.854E−01	5.886E−02	1
	f_{Ni}	3.293E−01	5.925E+00	3.560E+00	1.289E+00	0

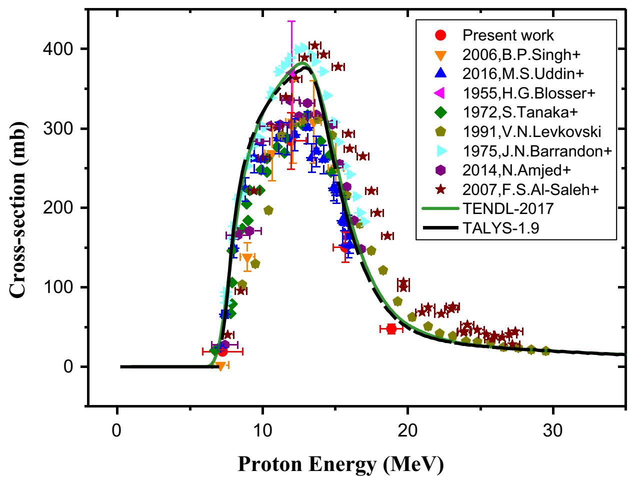

Fig. 1 Excitation function of $^{60}Ni(p,n)^{60}Cu$ reaction

Results and discussion

The radionuclide ^{60}Cu is a short-lived one, produced through the $^{60}Ni(p, n)^{60}Cu$ reaction and was identified by the most prominent γ-line of 1332.5 keV with branching intensity of 88%. The cross-sections for the $^{60}Ni(p,n)^{60}Cu$ reaction from threshold energy up to 18.88 ± 0.76 MeV proton energy are shown in Fig. 1 and are presented in Table 5 together with their uncertainties. The uncertainty in beam intensity as a result of uncertainties in counts, efficiency, time factors and was found to be 7.7%. The final uncertainty obtained in the $^{60}Ni(p,n)^{60}Cu$ reaction cross-section is found to be ~ 12.5%. In Fig. 1, the excitation function from the present work is compared with the available literature data [6–10] existing in EXFOR [12] database. The data of Levkovski were corrected as suggested by Qaim et al. [30]. It can be seen from Fig. 1 that the present data are in agreement with most of the literature data [6, 8–10]. In fact, the present experimental cross-sections confirm the data of Tanaka et al. [6], Uddin et al. [9] and Singh et al. [8]. Figure 1 also shows that the experimental data of the present work are acquired with less uncertainty as compared to those literature data by Blosser et al. [7] and Singh et al. [8]. In particular, the one datum point around the peak position reported by Blosser et al. [7] is significantly high with a large uncertainty.

In Fig. 1, three additional sets of data by Barrandon et al. [31], Amjed et al. [32] and Saleh et al. [33] were also included. These data were normalised from $^{nat}Ni(p,x)^{60}Cu$ reaction by simple scaling method based on the isotopic abundance of the target. The data by Barrandon et al. [31] and Saleh et al. [32] were found to be significantly high relative to other literature data, whereas the data by Amjed et al. [33] are in good agreement with other experimental data from EXFOR [12] database.

The excitation function of the $^{60}Ni(p,n)^{60}Cu$ reaction was obtained theoretically using the TALYS-1.9 code [13] with default parameters and then plotted in Fig. 1 together with data from TENDL-2017 library [14]. We have considered both TALYS code and TENDL-2017 library because it is not known which parameters and which version of the TALYS code were used for the values reported in TENDL-2017 library. The interplay between theory and experiment is vital in understanding the fundamental interaction between the projectile and target nuclei, and in obtaining accurate and reliable nuclear data. In this context, many theoretical nuclear codes like TALYS have been developed. TALYS [13] is a code which predicts the nuclear reaction of target nuclides with nuclear mass 12 or heavier, induced by particles of energy ranging from 1 keV to 200 MeV. In this code, Konig et al. [13] have executed a number of nuclear models, categorized into optical, direct, pre-equilibrium, compound and fission models, into a single code system. The nuclear data obtained from this nuclear code offer essential information that can be employed in various nuclear applications. TALYS-1.9 is the latest version of TALYS and is elaborated in detail in its manual [34].

It can be seen that the excitation functions of $^{60}Ni(p,n)^{60}Cu$ reaction from both TALYS-1.9 and TENDL-2017 data library follows the same trend as the experimental data from literature and present work. However, there is slight difference in the peak position of reaction cross-section between the values from TENDL-2017 library [14] and theoretical values based on TALYS-1.9 code [13]. This may be due to difference in the parameters or the old version of TALYS code used in TENDL data library. It can be also seen from Fig. 1 that the experimental data by Barrandon et al. [31], Saleh et al. [33] and the single datum reported by Blosser et al. [7] matches with the theoretical values. On the other hand, rest of the literature data [6, 8–10, 32] and present data, follows a particular trend and matches with the theoretical values from TALYS-1.9 and TENDL-2017 library at higher proton energy but not around peak position of the reaction cross-section. This indicates that, the theoretical calculation by TALYS-1.9 with default parameters has to be re-examine. Besides this, a proper knowledge of covariance analysis can help to improve the nuclear data and the results becomes more accurate when the final uncertainty are evaluated by taking into consideration the uncertainties that may arises from various sources of experimental errors.

Conclusion

The $^{60}Ni(p,n)^{60}Cu$ reaction cross sections from threshold energy to ~ 20 MeV have been measured by employing stack foil activation and off-line γ-ray spectrometric technique. The methodology of covariance matrix and least square methods have been employed in the efficiency calibration of HPGe detector and the uncertainty measurement of $^{60}Ni(p,n)^{60}Cu$ reaction cross-section. Our fitted cross-sections for the $^{60}Ni(p,n)^{60}Cu$ reaction are in acceptable agreement with most of the literature data. The present work confirms that a proper knowledge of uncertainty should be taken care to improve the nuclear data, which can be used in various fields of applications. It is more important to increase the measure of quality rather than of accuracy. Hence, a proper analysis of covariance is necessary to assess the quality of the results stated to meet the established accuracy requirements.

Acknowledgements We would like to express our sincere thanks to the staffs of Tata Institute Fundamental Research, Mumbai for their kind help and their excellent operation of the accelerator during irradiations. One of the authors (B. Lawriniang) also gratefully acknowledges the financial support of the UGC for her PhD work.

References

1. Cullen DE, Muranaka R, Schmidt J (1990) Reactor physics calculations for applications in nuclear technology. In: Proceedings of the workshop, Trieste, Italy, 12–16 Mar 990
2. Yigit M, Kara A (2017) Simulation study of the proton-induced reaction cross-sections for the production of ^{18}F and $^{66\text{-}68}Ga$ radioisotopes. J Radioanal Nucl Chem 314:2383–2392
3. Talou P, Chadwick MB, Young PG (2001) Recent developments in nuclear data for ADS T-16. Lectures given at the workshop on nuclear data for science and technology: accelerator driven waste incineration, Trieste, 10–21 Sept 2001
4. Enferadi M, Sarbazvatan S, Sadeghi M, Hong JH, Tung CJ, Chao TC, Lee CC, Wey SP (2017) Nuclear reaction cross sections for proton therapy applications. J Radioanal Nucl Chem 314:1207–1235
5. Bailey DL, Townsend DW, Valk PE, Maisey MN (2005) Positron emission tomography: basic Sciences, Springer. https://doi.org/10.1007/B136169
6. Tanaka S, Furukawa M, Chiba M (1972) Nuclear reactions of nickel with protons up to 56 MeV. J Inorg Nucl Chem 34:2419–2426
7. Blosser HG, Handley TH (1955) Survey of (p, n) reactions at 12 MeV. Phys Rev C 100(5):1340–1344
8. Singh BP, Sharma MK, Musthafa MM, Bhardwaj HD, Prasad R (2006) A study of pre-equilibrium emission in some proton- and alpha-induced reactions. Nucl Instrum Methods Phys Res, Sect A 562:717–720
9. Uddin MS, Sudar S, Spahn I, Shariff MA, Qaim SM (2016) Excitation function of the 60Ni(p, γ)61Cu reaction from threshold to 16 MeV. Phys Rev C 93:044606
10. Levkovskij VP, Reutov VF, Botvin KV (1990) Helium formation in molybdenum, zirconium, niobium, nickel, iron and chromium under irradiation by 8–30 MeV protons. At Ehnergiya 69(3):180–182
11. Sheela YS, Naik H, Prasad KM, Ganesan S, Nair NS, Suryanarayana SV (2017) Covariance analysis of efficiency calibration of HPGe detector internal report no. MU/STATISTICS/DAE-BRNS/2017/119-February-2017
12. IAEA-EXFOR Data base. http://www.nds.iaea.org/exfor. Accessed April 2018
13. Koning A, Hilaire S, Goriely S (2015) TALYS-1.8, A Nuclear Reaction Program, NRG-1755 ZG Petten. The Netherlands, http://www.talys.eu/download-talys. Accessed May 2018
14. Koning AJ, Rochman D (2012) Modern nuclear data evaluation with the TALYS code system. Nucl Data Sheets 113:2841–2934
15. Lawriniang B, Ghosh R, Badwar S, Vansola V, Sheela YS, Suryanarayana SV, Naik H, Naik YP, Jyrwa B (2018) Measurement of cross-sections for the $^{93}Nb(p,n)^{93m}Mo$ and $^{93}Nb(p,pn)^{92m}Nb$ reactions up to ~ 20 MeV energy. Nucl Physics A 973:79–88
16. BARC—TIFR Pelletron-LINAC facility silver, facility silver jubilee (1988 –2013)
17. http://www-nds.iaea.org/medical/monitor_reactions.html. Accessed April 2018
18. Tyler AW (1939) The beta- and gamma-radiations from copper^{64} and europium^{152}. Phys Rev 56(2):125–130
19. NuDat 2.7β (2011) National Nuclear Data Center, Brookhaven National Laboratory. https://www.nndc.bnl.gov/nudat2/. Accessed April 2018
20. https://www-nds.iaea.org/relnsd/vcharthtml/VChartHTML.html. Accessed April 2018
21. Q-value. https://cdfe.sinp.msu.ru/services/calc_thr/calc_thr.html. Accessed April 2018
22. Ziegler JF (2016) SRIM-2013. the stopping and range of ions in solids. Pergamon, New York
23. Ghosh R, Badwar S, Lawriniang B, Yerraguntla SS, Naik H, Naik Y, Suryanayana SV, Jyrwa B, Ganesan S (2017) Measurement of photo-neutron cross-sections of Gd and Ce using Bremsstrahlung with an end point energy of 10 MeV. J Radioanal Nucl Chem 314:1983–1990
24. Geraldo LP, Smith DL (1990) Covariance analysis and fitting of Germanium Gamma-ray detector efficiency calibration data. Nucl Instrum Methods Phys Res, Sect A 290:499–508
25. Smith DL (1993) A least squares computational "tool kit". Nuclear data and measurement series ANL/NDM-128 Engineering Physics Division, Argonne National Laboratory Argonne, U.S.A, available on https://inis.iaea.org/collection/NCLCollectionStore/_Public/25/011/25011948.pdf
26. Sheela YS, Naik H, Manjunatha Prasad K, Ganesan S, Suryanarayana SV (2017) Detailed data sets related to covariance analysis of the measurement of cross section of $^{59}Co(n, g)^{60}Co$ reaction cross section relative to the cross section $^{115}In(n,g)^{116m}In$, https://www.researchgate.net/publication/317240473. Accessed Oct 2017
27. Gilmore G, Hemingway JD (1995) Practical Gamma-Ray Spectrometry. John Wiley and Sons, England, p 17
28. Otuka N, Lalremruata B, Khandaker MU, Usman AR, Punte LRM (2017) Uncertainty propagation in activation cross section measurements. Radiat Phys Chem 140:502–510
29. Badwar S, Ghosh R, Yerraguntla SS, Jyrwa BM, Lawriniang BM, Naik H, Naik Y, Suryanarayana V, Ganesan S (2018) Measurements and uncertainty propagation for the natNi(p, x)61Cu reaction cross-section up to the proton energies of 20 MeV. Nucl Phys A 977:112–128
30. Qaim SM, Sudar S, Scholten A, Koning AJ, Coenen HH (2014) Evaluation of excitation functions of 100Mo(p, d + pn)99Mo and 100Mo (p,2n)99mTc reactions: estimation of long-lived Tc-impurity and its implication on the specific activity of cyclotron-produced 99mTc. Appl Radiat Isot 85:101–113
31. Barrandon JN, Debrun JL, Kohn A, Spear RH (1975) A study of the main radioisotopes obtained by irradiation of Ti, V, Cr, Fe, Ni, Cu and Zn with protons from 0 to 20 MeV. Nucl Instrum Methods 127:269–278
32. Amjed N, Tárkányi F, Hermanne A, Ditroi F, Takács S, Hussain M (2014) Activation cross-sections of proton induced reactions on natural Ni up to 65 MeV. Appl RadiatIsot 92:73–84
33. Al Saleh FS, Al Mugren KS, Azzam A (2007) Excitation functions of (p,x) reactions on natural nickel between proton energies of 2.7 and 27.5 MeV. Appl Radiat Isot 65(1):104–113
34. ftp://ftp.nrg.eu/pub/www/talys/talys1.9.pdf